

Nonreciprocal radiative heat transfer between two planar bodies

Lingling Fan¹,[✉] Yu Guo,¹ Georgia T. Papadakis,¹ Bo Zhao¹,[✉] Zhixin Zhao,¹ Siddharth Buddhiraju,¹ Meir Orenstein,² and Shanhui Fan^{1,*}

¹*Department of Electrical Engineering, Ginzton Laboratory, Stanford University, Stanford, California 94305, USA*

²*Department of Electrical Engineering, Technion-Israel Institute of Technology, 32000 Haifa, Israel*



(Received 21 October 2019; accepted 28 January 2020; published 7 February 2020)

We study the consequence of breaking reciprocity within the context of near-field radiative heat transfer between two planar bodies. Our findings introduce a thermodynamic constraint, which states that the heat transferred from one planar body to another at each frequency and in-plane wave vector is unchanged upon interchanging the two bodies, regardless of whether the materials are reciprocal or not. We further identify a unique signature of nonreciprocity, which is the breaking of the symmetry of the heat flux density between positive and negative in-plane wave vectors. We numerically demonstrate our findings in an example system consisting of magneto-optical materials. Our formalism applies to both near- and far-field regimes, opening opportunities for exploiting nonreciprocity in two-body radiative heat transfer systems.

DOI: [10.1103/PhysRevB.101.085407](https://doi.org/10.1103/PhysRevB.101.085407)

I. INTRODUCTION

Understanding radiative heat transfer [1–3] is essential in many applications ranging from radiative cooling [4–6] and thermal diodes [7] to thermal transistors [8–11] and thermophotovoltaic systems [12–16]. The majority of works investigating radiative heat transfer are limited to the materials that satisfy Lorentz reciprocity [17–30], and consequently the thermal emission and absorption are always equal according to Kirchhoff's law of thermal radiation [31]. The main characteristic for such reciprocal heat transfer is that the heat flux density map is symmetric for opposite in-plane wave vectors, both in far-field and near-field regimes. On the other hand, it is highly desirable to break the constraint of reciprocity in heat transfer between two bodies, as this is the key to reach thermodynamic limits in thermal radiation energy harvesting [32–34]. Therefore, in recent years there has been emerging interest in exploring radiative heat transfer with nonreciprocal materials. Examples include the design of photonic structures for complete violation of Kirchhoff's law in far-field thermal radiation [35,36], as well as the proposal for the thermal Hall effect [37], and persistent heat current in equilibrium in near-field heat transfer [38].

In an early paper [39], it was shown that the radiative heat transfer between two bodies in thermal equilibrium (same temperature) is symmetric even if the heat transfer is via a two-port nonreciprocal system (Faraday rotator). This result is equivalent to the lack of signature of nonreciprocity in this case. In [38], it was shown that this detailed balance can be violated for a nonreciprocal system, but it necessitates at least three bodies to generate a persistent current loop to maintain the equilibrium. In the current paper, we extend the results of [38,39] and show that detailed balance of heat transfer can be violated even between two bodies, provided that heat exchange can occur in more than one channel. We formally

prove and exemplify the result for heat transfer between two homogeneous infinite slabs, but the general consequence is by far more outreaching. For the two infinite slabs case, we show that heat transfer between body 1 and body 2 can occur in one channel while the inverse transfer occurs at a different one, and thus constitutes a persistent current loop between the two bodies. We show that the condition for this current loop is the violation of Lorenz reciprocity.

Our analytical results pertain to both far-field and near-field thermal radiation. We focus however on the near-field, where bodies are separated by a vacuum gap smaller than the thermal wavelength. The most studied geometry is that between two planar bodies (Fig. 1). Nevertheless, previous works on nonreciprocal near-field heat transfer have focused on nonplanar geometries [38,40,41]. There has not been a systematic study as to how nonreciprocity manifests itself in planar systems. Reference [42] considered near-field heat transfer between two planar structures incorporating magneto-optical materials. However, it did not address the manifestation of nonreciprocity, but rather demonstrated magnetic-field tuning of thermal radiation.

The paper is organized as follows: In Sec. II, we provide a derivation of the formalism for computing radiative heat transfer between two planar bodies. We place special emphasis on ensuring that it is applicable to both nonreciprocal and reciprocal systems. Using this formalism, in Secs. III and IV, we address how the second law of thermodynamics and reciprocity constrains near-field heat transfer in planar geometries. We highlight the uniquely nonreciprocal aspects of near-field heat transfer that cannot exist in reciprocal systems. In Sec. V, we provide numerical demonstrations of the theoretical predictions in Secs. III and IV. We conclude in Sec. VI.

II. THEORETICAL FORMALISM

Throughout the paper, we consider the general heat transfer setting as shown in Fig. 1. Body 1 and body 2 are

*shanhui@stanford.edu

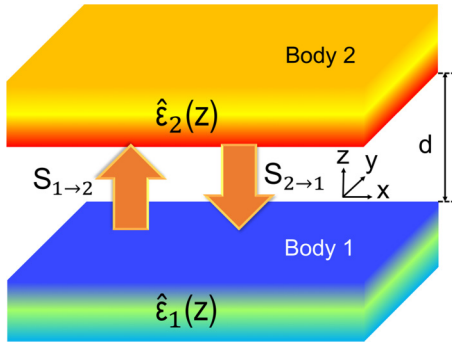


FIG. 1. Schematic of the geometry under consideration: Two semi-infinite planar slabs are separated by a vacuum gap of size d . Each slab has an in-plane (xy) homogeneous dielectric permittivity, which can be inhomogeneous in the z -direction, represented by the dielectric permittivity tensors $\hat{\epsilon}_1(z)$, $\hat{\epsilon}_2(z)$. $S_{1 \rightarrow 2}$ and $S_{2 \rightarrow 1}$ represent the radiative heat flux density from body 1 to 2 and body 2 to 1, respectively.

semi-infinite, separated by vacuum with a gap size of d , and maintained at temperatures T_1 and T_2 , respectively. Body 1 and 2 are described by a dielectric permittivity distribution $\hat{\epsilon}_1(z)$ and $\hat{\epsilon}_2(z)$, respectively, which are uniform in the in-plane directions, but can be nonuniform along the z -direction. In general, $\hat{\epsilon}_1(z)$, $\hat{\epsilon}_2(z)$ are 3×3 permittivity tensors. From the fluctuation dissipation theorem [43], the strength of the fluctuating current sources that generate thermal radiation is proportional to the imaginary part of the permittivity tensor, $\text{Im} \hat{\epsilon} \equiv \frac{1}{2j}(\hat{\epsilon} - \hat{\epsilon}^\dagger)$.

First, we compute the heat flux density from body 1 to body 2, $S_{1 \rightarrow 2}(\mathbf{r}_\parallel, z, t)$, which is defined as the absorbed power density in body 2 from the electric and magnetic field vectors $\mathbf{E}(\mathbf{r}_\parallel, z, t)$ and $\mathbf{H}(\mathbf{r}_\parallel, z, t)$ generated by the fluctuating current sources in body 1, and \mathbf{r}_\parallel , z , and t , are, respectively, the in-plane coordinate, distance along the vertical axis, and time. In the vacuum region between the two planar bodies in Fig. 1, the heat flux density from body 1 to 2, $S_{1 \rightarrow 2}(\mathbf{r}_\parallel, z, t)$ is equal to the ensemble-averaged z component of the Poynting vector, which is given by

$$S_{1 \rightarrow 2}(\mathbf{r}_\parallel, z, t) = \hat{\mathbf{z}} \cdot \langle \mathbf{E}(\mathbf{r}_\parallel, z, t) \times \mathbf{H}(\mathbf{r}_\parallel, z, t) \rangle, \quad (1)$$

where $\langle \dots \rangle$ represents an ensemble average. Throughout the paper, we adopt the following Fourier transformation conventions in time and space, respectively,

$$A(t) = \text{Re} \int_0^\infty d\omega A(\omega) e^{j\omega t}, \quad (2)$$

$$A(\mathbf{r}_\parallel) = \int \frac{d\mathbf{k}_\parallel}{(2\pi)^2} A(\mathbf{k}_\parallel) e^{-j\mathbf{k}_\parallel \cdot \mathbf{r}_\parallel}. \quad (3)$$

$S_{1 \rightarrow 2}(\mathbf{r}_\parallel, z, t)$ is independent of \mathbf{r}_\parallel by translational symmetry, independent of t since the thermal process is a stationary random process [44,45] and independent of z due to energy conservation as there is no absorption in the vacuum gap. Therefore, we have

$$\begin{aligned} & \langle \mathbf{E}(\mathbf{k}_\parallel, z, \omega) \times \mathbf{H}^*(\mathbf{k}'_\parallel, z, \omega') \rangle \\ &= \langle \mathbf{E}(\mathbf{k}_\parallel, z, \omega) \times \mathbf{H}^*(\mathbf{k}_\parallel, z, \omega) \rangle \delta(\mathbf{k}_\parallel - \mathbf{k}'_\parallel) \delta(\omega - \omega'), \quad (4) \end{aligned}$$

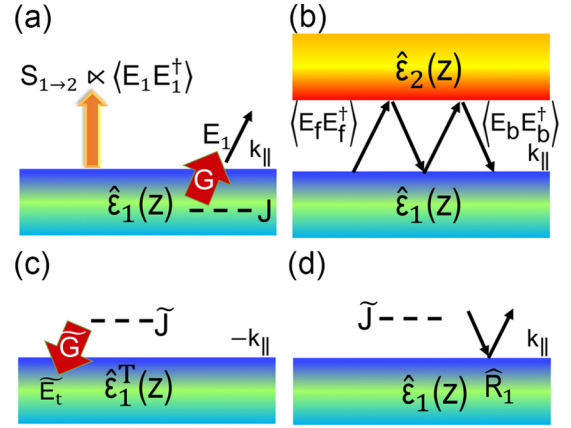


FIG. 2. Theoretical framework for computing the heat transfer in a two-body planar system using the generalized reciprocal relation. (a) Thermal emission of body 1. Poynting vector from body 1 to 2; $S_{1 \rightarrow 2}(\omega, \mathbf{k}_\parallel)$ is proportional to the electric field emission $\langle \mathbf{E}_1 \mathbf{E}_1^\dagger \rangle$ near the source surface. (b) Heat exchange between bodies 1 and 2 via multiple scattering process. Parts (c) and (d) illustrate the method to compute the field emission from a planar body using the generalized reciprocity relation. (c) The emission of body 1 can be equivalently computed by evaluating the absorption of the complementary body in the presence of the external source. (d) The absorption of the complementary body as shown in (c) can be computed in terms of its reflection coefficients.

where \mathbf{k}_\parallel , \mathbf{k}'_\parallel are the in-plane wave vector, and ω , ω' are the angular frequency. With these notations from Eqs. (1)–(4), we obtain

$$S_{1 \rightarrow 2} = \frac{1}{2} \text{Re} \int_0^\infty d\omega \int \frac{d\mathbf{k}_\parallel}{(2\pi)^4} \hat{\mathbf{z}} \cdot \langle \mathbf{E}(\mathbf{k}_\parallel, z, \omega) \times \mathbf{H}^*(\mathbf{k}_\parallel, z, \omega) \rangle. \quad (5)$$

Below we treat each \mathbf{k}_\parallel , ω component separately at a fixed z in the vacuum gap, and suppress the arguments of \mathbf{k}_\parallel , z , and ω .

We aim to express the near-field heat transfer between the two planar bodies, i.e., Eq. (5), in terms of the reflectivity matrix of each body. For this, we start by considering the electric field \mathbf{E}_1 as generated by body 1 in the absence of body 2 [Fig. 2(a)]. For propagating waves, defined by $k_\parallel < \frac{\omega}{c}$, where c is the speed of light in vacuum, immediately near the surface of body 1, the emitted field correlation is expressed as

$$\langle \mathbf{E}_1 \mathbf{E}_1^\dagger \rangle = (2\pi)^2 \frac{Z}{\pi} \Theta(\omega, T_1) [\hat{I} - \hat{R}_1 \hat{R}_1^\dagger], \quad (6)$$

whereas for evanescent waves with $k_\parallel > \frac{\omega}{c}$, we have

$$\langle \mathbf{E}_1 \mathbf{E}_1^\dagger \rangle = (2\pi)^2 \frac{Z}{\pi} \Theta(\omega, T_1) [\hat{R}_1 - \hat{R}_1^\dagger]. \quad (7)$$

In the Appendix, we provide an analytical derivation of Eqs. (6) and (7), based on the generalized reciprocity theorem [46]. $Z = \text{diag}(Z_s, Z_p)$, where Z_s and Z_p are the impedances for s - and p -polarized waves, defined to have the electric field or magnetic field parallel to the material interfaces, respectively. The function $\Theta(\omega, T)$ is the mean energy of photons per frequency ω at temperature T , defined as $\Theta(\omega, T) = \hbar\omega [\frac{1}{2} + \frac{1}{\exp(\hbar\omega/k_B T) - 1}]$. Here, \hbar is the reduced Planck constant,

and k_B is the Boltzmann constant. The reflectivity matrix of the i th body \hat{R}_i is given by

$$\hat{R}_i = \begin{bmatrix} R_i^{ss} & R_i^{sp} \\ R_i^{ps} & R_i^{pp} \end{bmatrix}, \quad (8)$$

where $R_i^{\sigma\mu}$ represents the reflection coefficient for light incident from vacuum into the i th body, with a μ -polarized incident wave and a σ -polarized reflected wave.

In the presence of body 2, the electric field between the two bodies, due to the thermal radiation from body 1, can be decomposed into forward and backward components [Fig. 2(b)], i.e., $\mathbf{E} = \mathbf{E}_f + \mathbf{E}_b$, which can be related to \mathbf{E}_1 as

$$\begin{aligned} \mathbf{E}_f &= \mathbf{E}_1 + \hat{R}_1 \hat{R}_2 e^{-j2k_z d} \mathbf{E}_1 + (\hat{R}_1 \hat{R}_2 e^{-j2k_z d})^2 \mathbf{E}_1 + \dots \\ &= \hat{D}_{12} \mathbf{E}_1, \end{aligned} \quad (9)$$

$$\mathbf{E}_b = \hat{R}_2 \hat{D}_{12} e^{-j2k_z d} \mathbf{E}_1 = \hat{D}_{21} \hat{R}_2 e^{-j2k_z d} \mathbf{E}_1, \quad (10)$$

where $\hat{D}_{mn} = [\hat{I} - \hat{R}_m \hat{R}_n e^{-j2k_z d}]^{-1}$ represents multiple reflections between the two bodies. In the alternative expression of \mathbf{E}_b , we have used the identity

$$\hat{R}_2 \hat{D}_{12} = \hat{D}_{21} \hat{R}_2. \quad (11)$$

Representing electric and magnetic fields by \mathbf{E}_f and \mathbf{E}_b , the averaged Poynting vector in Eq. (5) can then be written as

$$\frac{1}{2} \text{Re}\{\hat{\mathbf{z}} \cdot \langle \mathbf{E} \times \mathbf{H}^* \rangle\} = \frac{1}{2} \text{Re} \text{Tr}[(\mathbf{E}_f + \mathbf{E}_b)[Z^{-1}(\mathbf{E}_f - \mathbf{E}_b)]^\dagger], \quad (12)$$

which holds for propagating as well as evanescent modes, and \mathbf{E}_f and \mathbf{E}_b denote the forward and backward field components on the s - and p -polarization basis. Note that the basis vector for the p -polarization has opposite signs for forward and backward waves. For propagating waves, Eq. (12) becomes

$$\frac{1}{2} \text{Re}\{\hat{\mathbf{z}} \cdot \langle \mathbf{E} \times \mathbf{H}^* \rangle\} = \text{Tr} \left[\frac{1}{2Z} (\hat{I} - \hat{R}_2^\dagger \hat{R}_2) \hat{D}_{12} \langle \mathbf{E}_1 \mathbf{E}_1^\dagger \rangle \hat{D}_{12}^\dagger \right], \quad (13)$$

whereas for evanescent waves, Eq. (12) becomes

$$\frac{1}{2} \text{Re}\{\hat{\mathbf{z}} \cdot \langle \mathbf{E} \times \mathbf{H}^* \rangle\} = \text{Tr} \left[\frac{1}{2Z} (\hat{R}_2^\dagger - \hat{R}_2) \hat{D}_{12} \langle \mathbf{E}_1 \mathbf{E}_1^\dagger \rangle \hat{D}_{12}^\dagger e^{-2\alpha d} \right]. \quad (14)$$

In the latter case, the field components \mathbf{E}_f and \mathbf{E}_b denote exponential decay and growth, respectively, along the z^+ -direction, where $k_z = -j\alpha$, with α being the $1/e$ -penetration depth of the evanescent wave.

Plugging Eq. (6) and Eq. (7) into Eqs. (13) and (14), respectively, and by recalling Eq. (5), we obtain the total heat flux density from body 1 to body 2:

$$S_{1 \rightarrow 2} = \int_0^\infty \frac{d\omega}{2\pi} \int \frac{d\mathbf{k}_\parallel}{(2\pi)^2} \Theta(\omega, T_1) S_{1 \rightarrow 2}(\mathbf{k}_\parallel, \omega), \quad (15)$$

where $S_{1 \rightarrow 2}(\mathbf{k}_\parallel, \omega)$ is given by

$$\begin{aligned} S_{1 \rightarrow 2}(\mathbf{k}_\parallel, \omega) &= \text{Tr}\{[\hat{I} - \hat{R}_2^\dagger(\mathbf{k}_\parallel, \omega)\hat{R}_2(\mathbf{k}_\parallel, \omega)]\hat{D}_{12}(\mathbf{k}_\parallel, \omega) \\ &\times [\hat{I} - \hat{R}_1(\mathbf{k}_\parallel, \omega)\hat{R}_1^\dagger(\mathbf{k}_\parallel, \omega)]\hat{D}_{12}^\dagger(\mathbf{k}_\parallel, \omega)\} \end{aligned} \quad (16)$$

for propagating waves, and

$$\begin{aligned} S_{1 \rightarrow 2}(\mathbf{k}_\parallel, \omega) &= \text{Tr}\{[\hat{R}_2^\dagger(\mathbf{k}_\parallel, \omega) - \hat{R}_2(\mathbf{k}_\parallel, \omega)]\hat{D}_{12}(\mathbf{k}_\parallel, \omega) \\ &\times [\hat{R}_1(\mathbf{k}_\parallel, \omega) - \hat{R}_1^\dagger(\mathbf{k}_\parallel, \omega)]\hat{D}_{12}^\dagger(\mathbf{k}_\parallel, \omega)e^{-2\alpha d}\}, \end{aligned} \quad (17)$$

for evanescent waves. The heat flux density from body 2 to body 1 can be obtained from Eqs. (16) and (17) by exchanging the subscripts 1 and 2 and changing the temperature in Eq. (15) from T_1 to T_2 . We note that the derivation above does not assume reciprocity. This result is therefore generally applicable for either reciprocal or nonreciprocal systems. While this result was obtained [42] by integrating thermal sources in the emitting medium, here we show that it is a consequence of the generalized reciprocity theorem, which provides a direct relation between the scattering coefficients and the emissivity. Such an application of the generalized reciprocity theorem was not explicitly noted for nonreciprocal thermal emitters previously in the literature.

III. CONSTRAINT FROM THE SECOND LAW OF THERMODYNAMICS

In this section, we show that Eqs. (16) and (17) satisfy the second law of thermodynamics by showing that the heat flux from body 1 to body 2 is balanced with the heat flux from body 2 to body 1, at each frequency ω , and in-plane wave vector \mathbf{k}_\parallel , i.e.,

$$S_{1 \rightarrow 2}(\mathbf{k}_\parallel, \omega) = S_{2 \rightarrow 1}(\mathbf{k}_\parallel, \omega). \quad (18)$$

We start by providing a direct proof of Eq. (18) from Eqs. (16) and (17). For this purpose, we first state a few mathematical observations: We recall Eq. (11) above as well as the analogous relation:

$$\hat{R}_1 \hat{D}_{21} = \hat{D}_{12} \hat{R}_1. \quad (19)$$

By expanding \hat{D}_{12} , \hat{D}_{21} in series, we note that

$$\hat{D}_{12} = \hat{I} + \hat{R}_1 \hat{D}_{21} \hat{R}_2 e^{-j2k_z d}, \quad (20)$$

$$\hat{D}_{21} = \hat{I} + \hat{R}_2 \hat{D}_{12} \hat{R}_1 e^{-j2k_z d}. \quad (21)$$

First, we consider the case of propagating waves. The heat flux $S_{1 \rightarrow 2}(\mathbf{k}_\parallel, \omega)$ can be written as the sum of four terms, i.e.,

$$S_{1 \rightarrow 2}(\mathbf{k}_\parallel, \omega) = \mathcal{Z}_1 + \mathcal{Z}_2 + \mathcal{Z}_3 + \mathcal{Z}_4, \quad (22)$$

where

$$\mathcal{Z}_1 = -\text{Tr}[\hat{R}_2^\dagger \hat{R}_2 \hat{D}_{12} \hat{D}_{12}^\dagger] = -\text{Tr}[\hat{R}_2 \hat{D}_{12} \hat{D}_{12}^\dagger \hat{R}_2^\dagger], \quad (23)$$

$$\mathcal{Z}_2 = -\text{Tr}[\hat{D}_{12} \hat{R}_1 \hat{R}_1^\dagger \hat{D}_{12}^\dagger] = -\text{Tr}[\hat{R}_1 \hat{D}_{21} \hat{D}_{21}^\dagger \hat{R}_1^\dagger]. \quad (24)$$

From Eqs. (23) and (24), it can be shown that $\mathcal{Z}_1 + \mathcal{Z}_2$ is symmetric with respect to exchanging the subscripts 1 and 2. Furthermore, for the last two terms in Eq. (22), we can write

$$\begin{aligned} \mathcal{Z}_3 &= \text{Tr}[\hat{D}_{12} \hat{D}_{12}^\dagger] = \text{Tr}[\hat{I} + \hat{R}_1 \hat{D}_{21} \hat{R}_2 (\hat{R}_1 \hat{D}_{21} \hat{R}_2)^\dagger \\ &+ \text{Tr}[\hat{R}_1 \hat{D}_{21} \hat{R}_2 e^{-j2k_z d}] + \text{Tr}[\hat{R}_1 \hat{D}_{21} \hat{R}_2 e^{-j2k_z d}]^\dagger, \end{aligned} \quad (25)$$

$$\mathcal{Z}_4 = \text{Tr}[\hat{R}_2^\dagger \hat{R}_2 \hat{D}_{12} \hat{R}_1 \hat{R}_1^\dagger \hat{D}_{12}^\dagger] = \text{Tr}[\hat{R}_2 \hat{D}_{12} \hat{R}_1 (\hat{R}_2 \hat{D}_{12} \hat{R}_1)^\dagger]. \quad (26)$$

From Eqs. (25) and (26), $\mathcal{Z}_3 + \mathcal{Z}_4$ is also symmetric with respect to the subscript exchange between bodies 1 and 2. This can be seen by applying $\text{Tr}[\hat{R}_1\hat{D}_{21}\hat{R}_2] = \text{Tr}[\hat{R}_2\hat{D}_{12}\hat{R}_1]$ as derived from Eqs. (11) and (19). This proves Eq. (18) for propagating waves.

We now consider the case of evanescent waves, and we write $S_{1\rightarrow 2}(\mathbf{k}_{\parallel}, \omega)$ as a sum of four terms [Eq. (22)], where

$$\begin{aligned} \mathcal{Z}_1 &= \text{Tr}[\hat{R}_2^\dagger\hat{D}_{12}\hat{R}_1\hat{D}_{12}^\dagger]e^{-2\alpha d} \\ &= \text{Tr}[\hat{D}_{12}\hat{R}_1(\hat{R}_2\hat{D}_{12})^\dagger]e^{-2\alpha d}, \end{aligned} \quad (27)$$

$$\begin{aligned} \mathcal{Z}_2 &= \text{Tr}[\hat{R}_2\hat{D}_{12}\hat{R}_1^\dagger\hat{D}_{12}^\dagger]e^{-2\alpha d} \\ &= \text{Tr}[\hat{D}_{21}\hat{R}_2(\hat{R}_1\hat{D}_{21})^\dagger]e^{-2\alpha d}. \end{aligned} \quad (28)$$

From Eqs. (27) and (28), $\mathcal{Z}_1 + \mathcal{Z}_2$ remains symmetric with respect to the exchange between bodies 1 and 2. Furthermore,

$$\mathcal{Z}_3 = \text{Tr}[-\hat{R}_2\hat{D}_{12}\hat{R}_1\hat{D}_{12}^\dagger]e^{-2\alpha d} = \text{Tr}[-\hat{D}_{21}\hat{D}_{12}^\dagger + \hat{D}_{12}^\dagger], \quad (29)$$

$$\mathcal{Z}_4 = \text{Tr}[-\hat{R}_2^\dagger\hat{D}_{12}\hat{R}_1^\dagger\hat{D}_{12}^\dagger]e^{-2\alpha d} = \text{Tr}[-\hat{D}_{12}\hat{D}_{21}^\dagger + \hat{D}_{12}]. \quad (30)$$

It can therefore be seen that $\mathcal{Z}_3 + \mathcal{Z}_4$ is also symmetric with respect to exchanging bodies 1 and 2, using $\text{Tr}\hat{D}_{12} = \text{Tr}\hat{D}_{21}$ via Eqs. (20) and (21). This proves Eq. (18) at every frequency ω and in-plane wave vector \mathbf{k}_{\parallel} of evanescent waves. For a system where heat transfer occurs entirely between two bodies, in thermal equilibrium, the net heat flow between the two must be zero as dictated by the second law of thermodynamics, independent of whether the system is reciprocal or not [39]. Thus, we have proven here that Eqs. (16) and (17) obey the second law of thermodynamics, even in the presence of nonreciprocity. Furthermore, Eq. (18) represents a general constraint on the heat transfer between two planar bodies, which must be satisfied in both reciprocal and nonreciprocal systems.

IV. CONSTRAINT FROM RECIPROCITY

In this section, we show that in reciprocal systems, i.e., systems where both planar bodies consist of reciprocal materials, an additional constraint arises:

$$S_{1\rightarrow 2}(\mathbf{k}_{\parallel}, \omega) = S_{2\rightarrow 1}(-\mathbf{k}_{\parallel}, \omega). \quad (31)$$

To prove Eq. (31), we start by observing that the scattering matrix of a reciprocal system is symmetric [47]. Hence, its reflectivity matrix satisfies

$$\hat{R}_1(-\mathbf{k}_{\parallel}) = \hat{\sigma}_z \hat{R}_1^T(\mathbf{k}_{\parallel}) \hat{\sigma}_z, \quad (32)$$

where $\hat{\sigma}_z = \text{diag}[1, -1]$. Note that the matrix $\hat{\sigma}_z$ appears because the electric field components for the p -polarization acquire opposite signs for \mathbf{k}_{\parallel} and $-\mathbf{k}_{\parallel}$. Henceforth, the argument ω is suppressed for brevity since the derivation applies to each frequency separately. From Eq. (32), we have $\hat{D}_{12}(-\mathbf{k}_{\parallel}) = \hat{\sigma}_z \hat{D}_{21}^T(\mathbf{k}_{\parallel}) \hat{\sigma}_z$, as can be proved by inspecting \hat{D}_{12} and \hat{D}_{21} in the form of its series expansion.

Similar to the treatment in the previous section, we first consider propagating waves, for which

$$\begin{aligned} S_{1\rightarrow 2}(-\mathbf{k}_{\parallel}) &= \text{Tr} \left\{ \hat{\sigma}_z [\hat{I} - \hat{R}_2^*(\mathbf{k}_{\parallel}) \hat{R}_2^T(\mathbf{k}_{\parallel})] \hat{D}_{21}^T(\mathbf{k}_{\parallel}) \right. \\ &\quad \left. \times [\hat{I} - \hat{R}_1^T(\mathbf{k}_{\parallel}) \hat{R}_1^*(\mathbf{k}_{\parallel})] \hat{D}_{21}^*(\mathbf{k}_{\parallel}) \hat{\sigma}_z \right\} \end{aligned}$$

$$\begin{aligned} &= \text{Tr} \left\{ [\hat{I} - \hat{R}_1^\dagger(\mathbf{k}_{\parallel}) \hat{R}_1(\mathbf{k}_{\parallel})] \hat{D}_{21}(\mathbf{k}_{\parallel}) \right. \\ &\quad \left. \times [\hat{I} - \hat{R}_2(\mathbf{k}_{\parallel}) \hat{R}_2^\dagger(\mathbf{k}_{\parallel})] \hat{D}_{21}^\dagger(\mathbf{k}_{\parallel}) \right\} \\ &= S_{2\rightarrow 1}(\mathbf{k}_{\parallel}). \end{aligned} \quad (33)$$

Similarly, for evanescent waves, the following holds:

$$\begin{aligned} S_{1\rightarrow 2}(-\mathbf{k}_{\parallel}) &= \text{Tr} \left\{ \hat{\sigma}_z [\hat{R}_2^*(\mathbf{k}_{\parallel}) - \hat{R}_2^T(\mathbf{k}_{\parallel})] \hat{D}_{21}^T(\mathbf{k}_{\parallel}) \right. \\ &\quad \left. \times [\hat{R}_1^T(\mathbf{k}_{\parallel}) - \hat{R}_1^*(\mathbf{k}_{\parallel})] \hat{D}_{21}^*(\mathbf{k}_{\parallel}) \hat{\sigma}_z e^{-2\alpha d} \right\} \\ &= \text{Tr} \left\{ [\hat{R}_1^\dagger(\mathbf{k}_{\parallel}) - \hat{R}_1(\mathbf{k}_{\parallel})] \hat{D}_{21}(\mathbf{k}_{\parallel}) \right. \\ &\quad \left. \times [\hat{R}_2(\mathbf{k}_{\parallel}) - \hat{R}_2^\dagger(\mathbf{k}_{\parallel})] \hat{D}_{21}^\dagger(\mathbf{k}_{\parallel}) e^{-2\alpha d} \right\} \\ &= S_{2\rightarrow 1}(\mathbf{k}_{\parallel}). \end{aligned} \quad (34)$$

Hence, for any system consisting of two planar bodies, if Eq. (31) is violated, then Eq. (32) must also be violated for at least one of the bodies. Thus, at least one of the bodies must consist of a nonreciprocal material. Therefore, the violation of Eq. (31) is a uniquely nonreciprocal effect in heat transfer between planar bodies. We can refer to the violation of Eq. (31) as a definition of nonreciprocal heat transfer for planar systems. It should be noted that the incorporation of nonreciprocal media in the system does not necessarily lead to nonreciprocal heat transfer [42]. Namely, satisfying Eq. (31) does not guarantee that the underlying system is reciprocal. One can construct systems in which the reflectivity matrix of each individual body violates Eq. (32), and hence each individual body is nonreciprocal, but the resulting heat transfer is reciprocal—satisfying Eq. (31). We provide such an example in the numerical demonstration section below.

V. NUMERICAL DEMONSTRATIONS

In this section, we numerically demonstrate the findings of the previous sections. We perform numerical calculations of heat transfer between two planar slabs based on the formalism provided above. First, we consider a reciprocal system consisting of two planar slabs of reciprocal materials, as shown in Fig. 3(a). We set body 1 to have an isotropic dielectric permittivity, $\hat{\epsilon}_1 = \epsilon_p$, where ϵ_p is the dielectric function of a plasmonic metal that takes the Drude model form $\epsilon_p = 1 - \frac{\omega_p^2}{\omega(\omega + j/\tau)}$. ω_p is the plasma frequency, and $1/\tau = 0.1\omega_p$ characterizes the plasmonic scattering rate. We choose the permittivity of the second body to be anisotropic and have the form

$$\hat{\epsilon}_2^S(\omega) = \begin{bmatrix} \epsilon_p & 0 & 0 \\ 0 & \epsilon_d & \epsilon_f \\ 0 & \epsilon_f & \epsilon_d \end{bmatrix}, \quad (35)$$

with $\epsilon_d = 1 - \frac{\omega_p^2(1+j\frac{1}{\tau\omega})}{(\omega+j/\tau)^2 - \omega_B^2}$, $\epsilon_f = -\frac{\omega_B}{\omega} \frac{\omega_p^2}{(\omega+j/\tau)^2 - \omega_B^2}$. Here, $\omega_B = \frac{eB}{m}$ is chosen to be $\omega_B = 0.2\omega_p$, where e is the electron charge, m is the electron mass, and B is the external magnetic field directed along the x -axis. The permittivity form of Eq. (35) is chosen to facilitate the comparison to the nonreciprocal case, as we will show below. This form resembles the permittivity of a magnetized plasma, except that the permittivity tensor is symmetric and hence the material is reciprocal. We define the plasma wavelength $\lambda_p = 2\pi c/\omega_p$, and we set the thickness of both slabs as $d_s = \lambda_p$. The width of the vacuum gap between

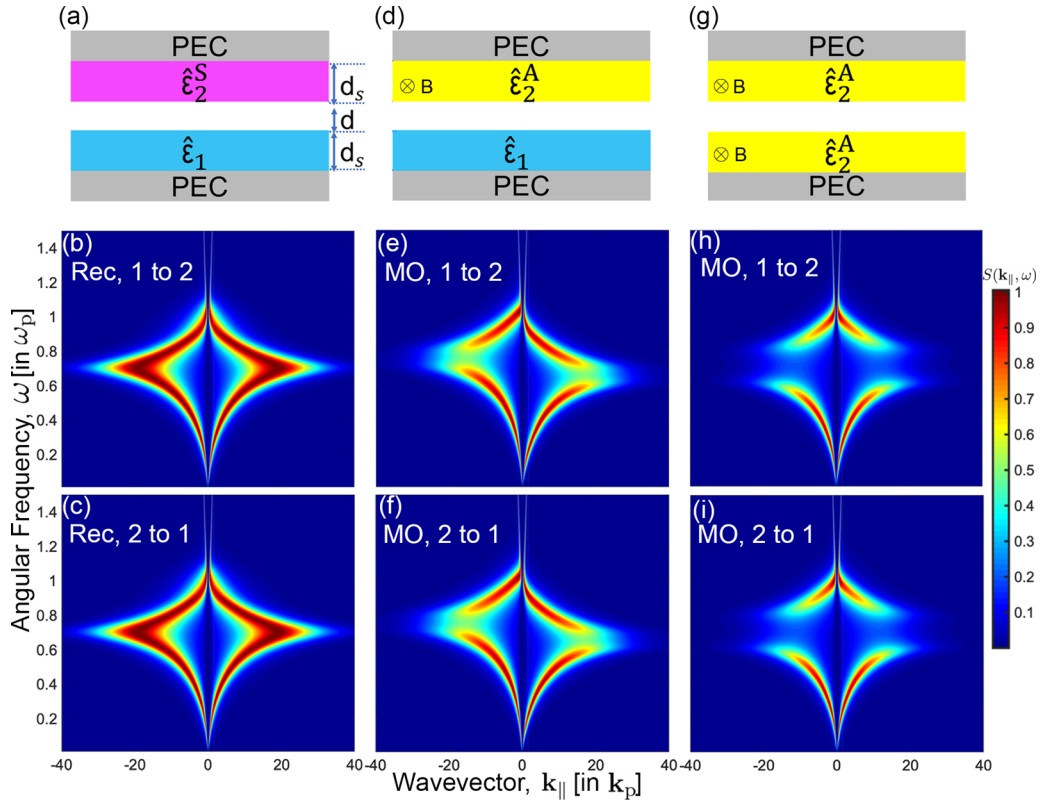


FIG. 3. Numerical simulations of heat transfer between two planar bodies at each frequency ω and in-plane wave vector \mathbf{k}_{\parallel} along the y -axis. Body 1 is an isotropic plasmonic medium in panels (a)–(f), and a magneto-optical material with an asymmetric permittivity tensor $[\hat{\epsilon}_2^A$ in Eq. (36)] in panels (g)–(i). Body 2 is an anisotropic material with a symmetric dielectric permittivity tensor $[\hat{\epsilon}_2^S$ in Eq. (35)] in panels (a)–(c), and a magneto-optical material with $\hat{\epsilon}_2^A$ [Eq. (36)] in panels (d)–(i). The thickness of the slabs is set to $d_s = \lambda_p$, whereas the vacuum gap has a width of $d = 0.1\lambda_p$, where λ_p is the bulk plasma wavelength. Panels (b), (e), and (h) represent the heat flux density from body 1 to 2, i.e., $S_{1 \rightarrow 2}$. Panels (c), (f), and (i) represent the heat flux density from body 2 to 1, i.e., $S_{2 \rightarrow 1}$. Panels (e) and (f) demonstrate the violation of reciprocity constraint for heat transfer, i.e., Eq. (31), whereas panels (b), (c) and (h), (i) satisfy Eq. (31). All results agree with the general thermodynamic constraint of Eq. (18).

two slabs is set to be $d = \lambda_p/10$ for probing near-field effects. To remove the effect of any bulk free-space propagating modes that occur at high frequencies, we place a perfect electric conductor (PEC) on the back side of both slabs.

Based on the formalism described in Sec. II, we compute the radiative heat transfer between these two bodies for the in-plane wave vector \mathbf{k}_{\parallel} along the y -direction, as shown in Figs. 3(b) and 3(c), corresponding to $S_{1 \rightarrow 2}(\mathbf{k}_{\parallel}, \omega)$ and $S_{2 \rightarrow 1}(\mathbf{k}_{\parallel}, \omega)$, respectively. We see that $S_{1 \rightarrow 2}(\mathbf{k}_{\parallel}, \omega) = S_{1 \rightarrow 2}(-\mathbf{k}_{\parallel}, \omega)$, as expected for a reciprocal system [Eq. (31)]. Furthermore, at each frequency and in-plane wave vector, we have $S_{1 \rightarrow 2}(\mathbf{k}_{\parallel}, \omega) = S_{2 \rightarrow 1}(\mathbf{k}_{\parallel}, \omega)$, confirming the validity of Eq. (18). We emphasize that these constraints are satisfied despite the lack of any mirror symmetry in the system. Bodies 1 and 2 are made of different materials, and moreover the permittivity of body 2 is chosen to be anisotropic such that different \mathbf{k}_{\parallel} are not equivalent. Next, we study a nonreciprocal case, where Eq. (31) is violated. We consider a system where body 1 remains the same as in the previous example, however body 2 has a permittivity tensor of the form [Fig. 3(d)]

$$\hat{\epsilon}_2^A(\omega) = \begin{bmatrix} \epsilon_p & 0 & 0 \\ 0 & \epsilon_d & j\epsilon_f \\ 0 & -j\epsilon_f & \epsilon_d \end{bmatrix}. \quad (36)$$

This permittivity tensor is asymmetric, thus breaking Lorentz reciprocity. The heat transfer spectra for this system are shown in Figs. 3(e) and 3(f). We see here that $S_{1 \rightarrow 2}(\mathbf{k}_{\parallel}, \omega) \neq S_{1 \rightarrow 2}(-\mathbf{k}_{\parallel}, \omega)$. Hence, based on the discussions in Sec. IV, we have shown that this system can achieve nonreciprocal near-field heat transfer in a planar geometry. This system, therefore, demonstrates a unique signature of nonreciprocity in the context of near-field heat transfer, as defined in the Introduction. Furthermore, by comparing Figs. 3(e) and 3(f), we see that $S_{1 \rightarrow 2}(\mathbf{k}_{\parallel}, \omega) = S_{2 \rightarrow 1}(\mathbf{k}_{\parallel}, \omega)$ for all frequencies ω and in-plane wave vectors \mathbf{k}_{\parallel} , in consistency with Eq. (18). This numerical example demonstrates that Eq. (18) is satisfied despite the lack of both reciprocity and mirror symmetry in the considered system.

Finally, we consider a nonreciprocal case, which demonstrates that even in the presence of nonreciprocity, Eq. (31) can hold. Hence, we set both bodies to have the permittivity tensor of Eq. (36). In this case, the signature of nonreciprocity by each individual body is canceled out via their combination. Consequently, we have $S_{1 \rightarrow 2}(\mathbf{k}_{\parallel}, \omega) = S_{1 \rightarrow 2}(-\mathbf{k}_{\parallel}, \omega)$ despite the fact that the response for each individual body is nonreciprocal. Furthermore, similar to the previous cases, the constraint $S_{1 \rightarrow 2}(\mathbf{k}_{\parallel}, \omega) = S_{2 \rightarrow 1}(\mathbf{k}_{\parallel}, \omega)$ is preserved since Fig. 3(h) is identical to Fig. 3(i),

once again verifying the general thermodynamic constraint Eq. (18).

The fluctuation dissipation theorem, as the theoretical basis for the formalism and numerical results given above, is known to agree with recent experiments [4,15,48–52], therefore demonstrating that geometrical and material imperfections [53] can be mitigated in near-field heat transfer. Potential experimental measurements of the nonreciprocity signature on the heat transfer could be facilitated since this signature translates into the symmetry breaking of the heat transfer function [Figs. 3(d) and 3(e)], which is measurable in principle. In the far-field, measuring the angular-spectral distribution of the heat flux uses configurations such as the Fourier optics setup [54–56]. In the near-field, such measurements are more involved, but significant steps toward their realization are in rapid progress (e.g., [57]).

To conclude this section, we provided a numerical demonstration showing that Eq. (18) holds both in reciprocal [Fig. 3(a)] and nonreciprocal systems [Figs. 3(d) and 3(g)]. Furthermore, we showed that the generalized detailed balance [Eq. (31)] holds for reciprocal systems, and the violation of Eq. (31) can only be achieved in nonreciprocal systems. Finally, we demonstrated a case in which Eq. (31) holds even when the underlying bodies are nonreciprocal.

VI. CONCLUSION

We presented a formalism for computing radiative heat transfer between two planar bodies. This formalism is applicable for both reciprocal and nonreciprocal systems. We introduced a constraint imposed by the second law of thermodynamics and reciprocity that holds at every in-plane wave vector and frequency [Eq. (18)]. Our formalism identifies the unique signature of nonreciprocity in heat transfer in two-body planar systems, in terms of breaking the symmetry between opposite-sign in-plane wave vectors in thermal transport [Figs. 3(e) and 3(f)].

ACKNOWLEDGMENTS

Discussions with L. Zhu and W. Jin are gratefully acknowledged. This work is supported by US Army Research Office (ARO) MURI Grant No. W911NF-19-1-0279. G.T.P. acknowledges the TomKat Postdoctoral Fellowship in Sustainable Energy at Stanford University. Z.Z. and S.B. acknowledge the support of a Stanford Graduate Fellowship.

APPENDIX

In this Appendix, we provide proof of Eqs. (6) and (7) presented in the main text regarding the fields emitted by a single planar body, based on the generalized reciprocity theorem. Equations (6) and (7) have been previously proven in Refs. [58–61] by using the second fluctuation-dissipation theorem, which directly relates the field emission to the imaginary part of the Green's function. The proof of Refs. [58–61] applies to both reciprocal and nonreciprocal systems. Here, we provide an alternative proof based entirely on the current correlation. This proof facilitates the understanding

of the differences between reciprocal and nonreciprocal systems.

We first summarize a few relations in electromagnetics that we will use below, applicable to reciprocal as well as nonreciprocal systems. For simplicity, for both theorems discussed below, we consider a nonmagnetic ($\mu = \mu_0$) system, described by relative dielectric permittivity $\hat{\epsilon}$.

Theorem 1. Conservation of energy. Let us consider a system that has two steady-state solutions as described by electric fields \mathbf{E}_σ and \mathbf{E}_μ . At each frequency ω , we have

$$\begin{aligned} & \int dV \omega \epsilon_0 \mathbf{E}_\sigma^* \cdot \left[\frac{\hat{\epsilon} - \hat{\epsilon}^\dagger}{2j} \right] \mathbf{E}_\mu \\ &= -\frac{1}{2} \int dS \hat{\mathbf{n}} \cdot (\mathbf{E}_\sigma^* \times \mathbf{H}_\mu + \mathbf{E}_\mu \times \mathbf{H}_\sigma^*). \end{aligned} \quad (\text{A1})$$

The proof of Eq. (A1) can be found in Ref. [62]. In the geometry of Fig. 2(a), where body 1 occupies the half-space $z < 0$, suppose that the fields $\mathbf{E}_\sigma(z)e^{-j\mathbf{k}_\parallel \cdot \mathbf{r}_\parallel}$, $\mathbf{H}_\sigma(z)e^{-j\mathbf{k}_\parallel \cdot \mathbf{r}_\parallel}$ and $\mathbf{E}_\mu(z)e^{-j\mathbf{k}_\parallel \cdot \mathbf{r}_\parallel}$, $\mathbf{H}_\mu(z)e^{-j\mathbf{k}_\parallel \cdot \mathbf{r}_\parallel}$ are solutions to Maxwell's equations at the in-plane wave vector \mathbf{k}_\parallel . Then, Eq. (A1) becomes

$$\begin{aligned} & \int_{-\infty}^0 dz \omega \epsilon_0 \mathbf{E}_\sigma^* \cdot \left[\frac{\hat{\epsilon} - \hat{\epsilon}^\dagger}{2j} \right] \mathbf{E}_\mu \\ &= -\frac{1}{2} (\mathbf{E}_\sigma^* \times \mathbf{H}_\mu + \mathbf{E}_\mu \times \mathbf{H}_\sigma^*) \cdot \hat{\mathbf{z}} |_{z=0^+}. \end{aligned} \quad (\text{A2})$$

Theorem 2. Generalized reciprocity theorem. For nonmagnetic systems, the electric field \mathbf{E} can be obtained by solving the equation $\nabla \times \nabla \times \mathbf{E} - k_0^2 \hat{\epsilon} \mathbf{E} = -j\omega \mu_0 \mathbf{J}$, where $k_0 = \omega/c$ and \mathbf{J} is the current density. The Green's function for this system is defined by

$$\nabla \times \nabla \times G - k_0^2 \hat{\epsilon} G = \mathbb{I} \delta(\mathbf{r} - \mathbf{r}'), \quad (\text{A3})$$

where \mathbb{I} is the identity dyad. The generalized reciprocity theorem states

$$\tilde{G}(\mathbf{r}', \mathbf{r}) = G^T(\mathbf{r}, \mathbf{r}'), \quad (\text{A4})$$

where \tilde{G} is the Green's function of its complementary system described by a permittivity of $\hat{\epsilon}^T$. For reciprocal systems, $\hat{\epsilon} = \hat{\epsilon}^T$, and hence $G(\mathbf{r}', \mathbf{r}) = G^T(\mathbf{r}, \mathbf{r}')$. The proof of Eq. (A4) closely parallels the standard proof in reciprocal systems, and can be found in Ref. [46].

Next, we consider the field emission in Eqs. (6) and (7). For the system shown in Fig. 2, by taking the Fourier transform of \tilde{G} and G , we obtain

$$\tilde{G}(\mathbf{k}_\parallel, z', z_0) = G^T(-\mathbf{k}_\parallel, z_0, z'). \quad (\text{A5})$$

For the system shown in Fig. 2(a), we calculate the electric field emission of $\mathbf{E}_1(\mathbf{k}_\parallel, z, \omega)$ near the surface $z = 0^+ \equiv z_0$. Using the relation $\mathbf{E}(\mathbf{r}) = -j\omega \mu_0 \int d\mathbf{r}' G(\mathbf{r}, \mathbf{r}') \cdot \mathbf{J}(\mathbf{r}')$, as well as the fluctuation dissipation theorem [2], which takes the following form:

$$\begin{aligned} & \langle \mathbf{J}(\mathbf{k}_\parallel, \omega, z) \mathbf{J}^\dagger(\mathbf{k}', \omega, z') \rangle \\ &= (2\pi)^2 \frac{4}{\pi} \omega \epsilon_0 \Theta(\omega, T) \left[\frac{\hat{\epsilon} - \hat{\epsilon}^\dagger}{2j} \right] \delta(\mathbf{k}_\parallel - \mathbf{k}'_\parallel) \delta(z - z'), \end{aligned} \quad (\text{A6})$$

we obtain the electric field emission in Eqs. (6) and (7) in the following form:

$$\begin{aligned}
\langle \mathbf{E}_1 \mathbf{E}_1^\dagger \rangle &= (\omega \mu_0)^2 \int dz' \int dz'' G(\mathbf{k}_\parallel, z_0, z') \\
&\quad \times \langle \mathbf{J}(\mathbf{k}_\parallel, \omega, z') \mathbf{J}^\dagger(\mathbf{k}_\parallel, \omega, z'') \rangle G^\dagger(\mathbf{k}_\parallel, z_0, z'') \\
&= (2\pi)^2 \frac{4}{\pi} \Theta(\omega, T) (\omega \mu_0)^2 \\
&\quad \times \int_{-\infty}^0 dz' \omega \epsilon_0 G(\mathbf{k}_\parallel, z_0, z') \left[\frac{\hat{\epsilon} - \hat{\epsilon}^\dagger}{2j} \right] G^\dagger(\mathbf{k}_\parallel, z_0, z') \\
&= (2\pi)^2 \frac{4}{\pi} \Theta(\omega, T) (\omega \mu_0)^2 \\
&\quad \times \left[\int_{-\infty}^0 dz' \omega \epsilon_0 \tilde{G}^\dagger(-\mathbf{k}_\parallel, z', z_0) \left[\frac{\tilde{\epsilon} - \tilde{\epsilon}^\dagger}{2j} \right] \tilde{G}(-\mathbf{k}_\parallel, z', z_0) \right]^T, \tag{A7}
\end{aligned}$$

where in the last step we have used generalized reciprocity as described in Eq. (A5). Here, the electric field \mathbf{E}_1 is expressed as $\mathbf{E}_1 = E_{1s}\mathbf{s} + E_{1p}\mathbf{p}_+$, where \mathbf{s} and \mathbf{p}_+ are the polarization unit vectors for the s - and p -polarized reflected waves, in consistency with the definition of the reflectivity matrix in Eq. (8). For subsequent use, we also define \mathbf{p}_- as the unit polarization vector for the incoming p -polarized wave.

The Green's function $\tilde{G}(-\mathbf{k}_\parallel, z', z_0)$ for the complementary system $\tilde{\epsilon} = \hat{\epsilon}^T$ takes the dyadic form $\tilde{G}(-\mathbf{k}_\parallel, z', z_0) = \frac{1}{-j\omega\mu_0} [\tilde{\mathbf{E}}_s \tilde{\mathbf{s}} + \tilde{\mathbf{E}}_p \tilde{\mathbf{p}}_-]$. Here, $\tilde{\mathbf{E}}_{s,p}$ stand for the electric field at z' , generated from s - or p -polarized current source at z_0 with unit amplitude in the complementary system. We define the polarization basis vectors $\tilde{\mathbf{s}}, \tilde{\mathbf{p}}_+, \tilde{\mathbf{p}}_-$ equivalently to $\mathbf{s}, \mathbf{p}_+, \mathbf{p}_-$, but for the in-plane wave vector $-\mathbf{k}_\parallel$. The polarization basis vectors are connected via $\tilde{\mathbf{s}} = -\mathbf{s}$, $\tilde{\mathbf{p}}_+ = \mathbf{p}_-$, $\tilde{\mathbf{p}}_- = \mathbf{p}_+$. In terms of the polarization basis $\tilde{\mathbf{s}}$ and $\tilde{\mathbf{p}}_-$, Eq. (A7) is expanded into four terms:

$$\begin{aligned}
\langle \mathbf{E}_1 \mathbf{E}_1^\dagger \rangle &= (2\pi)^2 \frac{4}{\pi} \Theta(\omega, T) (F_{ss} \tilde{\mathbf{s}} \tilde{\mathbf{s}}^\dagger + F_{sp} \tilde{\mathbf{p}}_- \tilde{\mathbf{s}}^\dagger + F_{ps} \tilde{\mathbf{s}} \tilde{\mathbf{p}}_-^\dagger \\
&\quad + F_{pp} \tilde{\mathbf{p}}_- \tilde{\mathbf{p}}_-^\dagger), \tag{A8}
\end{aligned}$$

where

$$\begin{aligned}
F_{\sigma\mu} &= \int_{-\infty}^0 dz' \omega \epsilon_0 \tilde{\mathbf{E}}_\sigma^* \cdot \left[\frac{\hat{\epsilon} - \hat{\epsilon}^\dagger}{2j} \right] \tilde{\mathbf{E}}_\mu \\
&= -\frac{1}{2} (\tilde{\mathbf{E}}_\sigma^* \times \tilde{\mathbf{H}}_\mu + \tilde{\mathbf{E}}_\mu \times \tilde{\mathbf{H}}_\sigma^*) \cdot \hat{\mathbf{z}} \Big|_{z=z_0}. \tag{A9}
\end{aligned}$$

On the other hand, $\tilde{\mathbf{E}}_s = -\frac{\omega\mu_0}{2k_z} [(1 + \tilde{R}_1^{ss})\tilde{\mathbf{s}} + \tilde{R}_1^{ps}\tilde{\mathbf{p}}_+]$, $\tilde{\mathbf{E}}_p = -\frac{\omega\mu_0}{2k_z} [\tilde{R}_1^{sp}\tilde{\mathbf{s}} + \tilde{\mathbf{p}}_- + \tilde{R}_1^{pp}\tilde{\mathbf{p}}_+]$ are the electric fields near the surface $z = z_0 \equiv 0^+$. The magnetic fields can be computed to be $\tilde{\mathbf{H}}_s = -\frac{k_0}{2k_z} [-\tilde{\mathbf{p}}_- - \tilde{R}_1^{ss}\tilde{\mathbf{p}}_+ + \tilde{R}_1^{ps}\tilde{\mathbf{s}}]$ and $\tilde{\mathbf{H}}_p = -\frac{k_0}{2k_z} [-\tilde{R}_1^{sp}\tilde{\mathbf{p}}_+ + \tilde{\mathbf{s}} + \tilde{R}_1^{pp}\tilde{\mathbf{s}}]$. By evaluating the right-hand side of Eq. (A9), we obtain the following relation for propagating waves:

$$\begin{aligned}
4F/Z &= (1 - |\tilde{R}_1^{ss}|^2 - |\tilde{R}_1^{ps}|^2) \mathbf{s} \mathbf{s}^\dagger + (\tilde{R}_1^{sp*} \tilde{R}_1^{ss} + \tilde{R}_1^{ps} \tilde{R}_1^{pp*}) \mathbf{s} \mathbf{p}_+^\dagger \\
&\quad + (\tilde{R}_1^{sp} \tilde{R}_1^{ss*} + \tilde{R}_1^{ps*} \tilde{R}_1^{pp}) \mathbf{p}_+ \mathbf{s}^\dagger \\
&\quad + (1 - |\tilde{R}_1^{pp}|^2 - |\tilde{R}_1^{ps}|^2) \mathbf{p}_+ \mathbf{p}_+^\dagger, \tag{A10}
\end{aligned}$$

whereas for evanescent waves, we have

$$\begin{aligned}
4F/Z &= (\tilde{R}_1^{ss} - \tilde{R}_1^{ss*}) \mathbf{s} \mathbf{s}^\dagger - (\tilde{R}_1^{ps*} - \tilde{R}_1^{ps}) \mathbf{s} \mathbf{p}_+^\dagger \\
&\quad - (\tilde{R}_1^{sp} - \tilde{R}_1^{sp*}) \mathbf{p}_+ \mathbf{s}^\dagger + (\tilde{R}_1^{pp} - \tilde{R}_1^{pp*}) \mathbf{p}_+ \mathbf{p}_+^\dagger. \tag{A11}
\end{aligned}$$

Here, the reflectivity matrix \tilde{R}_1 corresponds to the complementary system with $\tilde{\epsilon}$ at the in-plane vector $-\mathbf{k}_\parallel$, in the form of Eq. (8). We also note that $Z = \text{diag}[Z_s, Z_p]$, $Z_s = Z_p = Z_0 \frac{k_0}{k_z}$, and $Z_0 = \sqrt{\frac{\mu_0}{\epsilon_0}}$ is the impedance in vacuum. The reflectivity matrix \hat{R}_1 of the original system with $\hat{\epsilon}$ at \mathbf{k}_\parallel is related to \tilde{R}_1 in the complementary system with $\tilde{\epsilon}$ at $-\mathbf{k}_\parallel$ via $\tilde{R}_1(-\mathbf{k}_\parallel) = \hat{\sigma}_z \hat{R}_1^T(\mathbf{k}_\parallel) \hat{\sigma}_z$, as can be proved via symmetry by rotating the coordinate axes to transform the dielectric permittivity tensor [47]. Also, by recalling that $\hat{R}_1 = R_1^{ss} \mathbf{s} \mathbf{s} + R_1^{sp} \mathbf{s} \mathbf{p}_+ + R_1^{ps} \mathbf{p}_+ \mathbf{s} + R_1^{pp} \mathbf{p}_+ \mathbf{p}_+$, we express the field emission in Eq. (A8) as

$$\begin{aligned}
\langle \mathbf{E}_1 \mathbf{E}_1^\dagger \rangle &= (2\pi)^2 \frac{Z}{\pi} \Theta(\omega, T_1) \\
&\quad \times \begin{cases} [\hat{I} - \hat{R}_1 \hat{R}_1^\dagger], & \text{propagating waves,} \\ [\hat{R}_1 - \hat{R}_1^\dagger], & \text{evanescent waves.} \end{cases} \tag{A12}
\end{aligned}$$

We note that the derivation above does not use reciprocity, and hence is applicable to both reciprocal and nonreciprocal systems.

- [1] D. Polder and M. Van Hove, Theory of radiative heat transfer between closely spaced bodies, *Phys. Rev. B* **4**, 3303 (1971).
- [2] S. M. Rytov, Y. A. Kravtsov, and V. I. Tatarskii, *Principles of Statistical Radiophysics 4 - Wave Propagation Through Random Media* (Springer-Verlag, Berlin, 1989), Vol. X, p. 188.
- [3] J.-P. Mulet, K. Joulain, R. Carminati, and J.-J. Greffet, Enhanced radiative heat transfer at nanometric distances, *Microscale Thermophys. Eng.* **6**, 209 (2002).
- [4] B. Guha, C. Otey, C. B. Poitras, S. Fan, and M. Lipson, Near-field radiative cooling of nanostructures, *Nano Lett.* **12**, 4546 (2012).

- [5] A. P. Raman, M. A. Anoma, L. Zhu, E. Rephaeli, and S. Fan, Passive radiative cooling below ambient air temperature under direct sunlight, *Nature (London)* **515**, 540 (2014).
- [6] K. Chen, P. Santhanam, S. Sandhu, L. Zhu, and S. Fan, Heat-flux control and solid-state cooling by regulating chemical potential of photons in near-field electromagnetic heat transfer, *Phys. Rev. B* **91**, 134301 (2015).
- [7] C. R. Otey, W. T. Lau, and S. Fan, Thermal Rectification Through Vacuum, *Phys. Rev. Lett.* **104**, 154301 (2010).
- [8] B. Li, L. Wang, and G. Casati, Negative differential thermal resistance and thermal transistor, *Appl. Phys. Lett.* **88**, 143501 (2006).

- [9] N. Li, J. Ren, L. Wang, G. Zhang, P. Hänggi, and B. Li, Colloquium: Phononics: Manipulating heat flow with electronic analogs and beyond, *Rev. Mod. Phys.* **84**, 1045 (2012).
- [10] P. Ben-Abdallah and S.-A. Biehs, Near-Field Thermal Transistor, *Phys. Rev. Lett.* **112**, 044301 (2014).
- [11] I. Latella, O. Marconot, J. Sylvestre, L. G. Fréchet, and P. Ben-Abdallah, Dynamical Response of a Radiative Thermal Transistor Based on Suspended Insulator-Metal-Transition Membranes, *Phys. Rev. Appl.* **11**, 024004 (2019).
- [12] I. Celanovic, F. O’Sullivan, M. Ilak, J. Kassakian, and D. Perreault, Design and optimization of one-dimensional photonic crystals for thermophotovoltaic applications, *Opt. Lett.* **29**, 863 (2004).
- [13] E. Nefzaoui, J. Drevillon, and K. Joulain, Selective emitters design and optimization for thermophotovoltaic applications, *J. Appl. Phys.* **111**, 084316 (2012).
- [14] C. Simovski, S. Maslovski, I. Nefedov, and S. Tretyakov, Optimization of radiative heat transfer in hyperbolic metamaterials for thermophotovoltaic applications, *Opt. Express* **21**, 14988 (2013).
- [15] A. Fiorino, L. Zhu, D. Thompson, R. Mittapally, P. Reddy, and E. Meyhofer, Nanogap near-field thermophotovoltaics, *Nat. Nanotechnol.* **13**, 806 (2018).
- [16] Z. Omair, G. Scranton, L. M. Pazos-Outón, T. P. Xiao, M. A. Steiner, V. Ganapati, P. F. Peterson, J. Holzrichter, H. Atwater, and E. Yablonovitch, Ultraefficient thermophotovoltaic power conversion by band-edge spectral filtering, *Proc. Natl. Acad. Sci. (USA)* **116**, 15356 (2019).
- [17] S.-A. Biehs, F. S. S. Rosa, and P. Ben-Abdallah, Modulation of near-field heat transfer between two gratings, *Appl. Phys. Lett.* **98**, 243102 (2011).
- [18] Y. Guo, C. L. Cortes, S. Molesky, and Z. Jacob, Broadband super-planckian thermal emission from hyperbolic metamaterials, *Appl. Phys. Lett.* **101**, 131106 (2012).
- [19] O. Ilic, M. Jablan, J. D. Joannopoulos, I. Celanovic, H. Buljan, and M. Soljačić, Near-field thermal radiation transfer controlled by plasmons in graphene, *Phys. Rev. B* **85**, 155422 (2012).
- [20] M. Krüger, G. Bimonte, T. Emig, and M. Kardar, Trace formulas for nonequilibrium Casimir interactions, heat radiation, and heat transfer for arbitrary objects, *Phys. Rev. B* **86**, 115423 (2012).
- [21] Y. Guo and Z. Jacob, Thermal hyperbolic metamaterials, *Opt. Express* **21**, 15014 (2013).
- [22] O. D. Miller, S. G. Johnson, and A. W. Rodriguez, Effectiveness of Thin Films in Lieu of Hyperbolic Metamaterials in the Near Field, *Phys. Rev. Lett.* **112**, 157402 (2014).
- [23] B. Zhao, B. Guizal, Z. M. Zhang, S. Fan, and M. Antezza, Near-field heat transfer between graphene/hbn multilayers, *Phys. Rev. B* **95**, 245437 (2017).
- [24] V. Fernández-Hurtado, F. J. García-Vidal, S. Fan, and J. C. Cuevas, Enhancing Near-Field Radiative Heat Transfer with Si-Based Metasurfaces, *Phys. Rev. Lett.* **118**, 203901 (2017).
- [25] O. D. Miller, O. Ilic, T. Christensen, M. T. H. Reid, H. A. Atwater, J. D. Joannopoulos, M. Soljačić, and S. G. Johnson, Limits to the optical response of graphene and two-dimensional materials, *Nano Lett.* **17**, 5408 (2017).
- [26] L. Ge, Y. Cang, K. Gong, L. Zhou, D. Yu, and Y. Luo, Control of near-field radiative heat transfer based on anisotropic 2d materials, *AIP Adv.* **8**, 085321 (2018).
- [27] Y. Zhang, H.-L. Yi, and H.-P. Tan, Near-field radiative heat transfer between black phosphorus sheets via anisotropic surface plasmon polaritons, *ACS Photon.* **5**, 3739 (2018).
- [28] H. Wu, Y. Huang, L. Cui, and K. Zhu, Active Magneto-Optical Control of Near-Field Radiative Heat Transfer Between Graphene Sheets, *Phys. Rev. Appl.* **11**, 054020 (2019).
- [29] H. Shim, L. Fan, S. G. Johnson, and O. D. Miller, Fundamental Limits to Near-Field Optical Response Over Any Bandwidth, *Phys. Rev. X* **9**, 011043 (2019).
- [30] Y. H. Kan, C. Y. Zhao, and Z. M. Zhang, Near-field radiative heat transfer in three-body systems with periodic structures, *Phys. Rev. B* **99**, 035433 (2019).
- [31] G. Kirchhoff, Ueber das verhältniss zwischen dem emmissionsvermögen und dem absorptionsvermögen der körper für wärme und licht, *Ann. Phys.* **185**, 275 (1860).
- [32] P. T. Landsberg and G. Tonge, Thermodynamic energy conversion efficiencies, *J. Appl. Phys.* **51**, R1 (1980).
- [33] H. Ries, Complete and reversible absorption of radiation, *Appl. Phys. B* **32**, 153 (1983).
- [34] M. A. Green, Time-asymmetric photovoltaics, *Nano Lett.* **12**, 5985 (2012).
- [35] L. Zhu and S. Fan, Near-complete violation of detailed balance in thermal radiation, *Phys. Rev. B* **90**, 220301(R) (2014).
- [36] B. Zhao, Y. Shi, J. Wang, Z. Zhao, N. Zhao, and S. Fan, Near-complete violation of kirchhoff’s law of thermal radiation with a 0.3 tesla magnetic field, *Opt. Lett.* **44**, 4203 (2019).
- [37] P. Ben-Abdallah, Photon Thermal Hall Effect, *Phys. Rev. Lett.* **116**, 084301 (2016).
- [38] L. Zhu and S. Fan, Persistent Directional Current at Equilibrium in Nonreciprocal Many-Body Near Field Electromagnetic Heat Transfer, *Phys. Rev. Lett.* **117**, 134303 (2016).
- [39] Rayleigh, On the magnetic rotation of light and the second law of thermo-dynamics, *Nature (London)* **64**, 577 (1901).
- [40] L. Zhu, Y. Guo, and S. Fan, Theory of many-body radiative heat transfer without the constraint of reciprocity, *Phys. Rev. B* **97**, 094302 (2018).
- [41] C. Guo, Y. Guo, and S. Fan, Relation between photon thermal Hall effect and persistent heat current in nonreciprocal radiative heat transfer, *Phys. Rev. B* **100**, 205416 (2019).
- [42] E. Moncada-Villa, V. Fernández-Hurtado, F. J. García-Vidal, A. García-Martín, and J. C. Cuevas, Magnetic field control of near-field radiative heat transfer and the realization of highly tunable hyperbolic thermal emitters, *Phys. Rev. B* **92**, 125418 (2015).
- [43] L. Landau, E. Lifshitz, and L. Pitaevskii, *Course of Theoretical Physics* (Pergamon, New York, 1980), Pt. 2, Chap. VIII, Vol. 9.
- [44] L. Landau, E. Lifshitz, and L. Pitaevskii, *Statistical Physics*, 3rd ed., (Pergamon, Oxford, 1980), Pt. 1, Chap. XII and Pt. 2, Chap. VIII.
- [45] S. M. Rytov, Y. A. Kravtsov, and V. I. Tatarskii, *Principles of Statistical Radiophysics* (Springer-Verlag, Berlin, 1980), Chap. 3, Vol. 3.
- [46] J. A. Kong, *Electromagnetic Wave Theory*, 2nd ed. (Wiley, New York, 1990), pp. 404–411.
- [47] H. A. Haus, *Waves and Fields in Optoelectronics* (Prentice-Hall, Englewood Cliffs, NJ, 1984).
- [48] K. Kim, B. Song, V. Fernández-Hurtado, W. Lee, W. Jeong, L. Cui, D. Thompson, J. Feist, M. T. H. Reid, F. J. García-Vidal, J. C. Cuevas, E. Meyhofer, and P. Reddy, Radiative heat transfer in the extreme near field, *Nature (London)* **528**, 387 (2015).

- [49] R. St-Gelais, L. Zhu, S. Fan, and M. Lipson, Near-field radiative heat transfer between parallel structures in the deep subwavelength regime, *Nat. Nanotechnol.* **11**, 515 (2016).
- [50] B. Song, D. Thompson, A. Fiorino, Y. Ganjeh, P. Reddy, and E. Meyhofer, Radiative heat conductances between dielectric and metallic parallel plates with nanoscale gaps, *Nat. Nanotechnol.* **11**, 509 (2016).
- [51] R. St-Gelais, G. R. Bhatt, L. Zhu, S. Fan, and M. Lipson, Hot carrier-based near-field thermophotovoltaic energy conversion, *ACS Nano* **11**, 3001 (2017).
- [52] A. Fiorino, D. Thompson, L. Zhu, B. Song, P. Reddy, and E. Meyhofer, Giant enhancement in radiative heat transfer in sub-30 nm gaps of plane parallel surfaces, *Nano Lett.* **18**, 3711 (2018).
- [53] A. A. Sokolsky and M. A. Gorlach, Scaling laws, pressure anisotropy, and thermodynamic effects for blackbody radiation in a finite cavity, *Phys. Rev. A* **89**, 013847 (2014).
- [54] J. Le Gall, M. Olivier, and J.-J. Greffet, Experimental and theoretical study of reflection and coherent thermal emission by a sic grating supporting a surface-phonon polariton, *Phys. Rev. B* **55**, 10105 (1997).
- [55] H. Sai, Y. Kanamori, and H. Yugami, High-temperature resistive surface grating for spectral control of thermal radiation, *Appl. Phys. Lett.* **82**, 1685 (2003).
- [56] A. Vega-Flick, R. A. Duncan, J. K. Eliason, J. Cuffe, J. A. Johnson, J.-P. M. Peraud, L. Zeng, Z. Lu, A. A. Maznev, E. N. Wang, J. J. Alvarado-Gil, M. Sledzinska, C. M. Sotomayor Torres, G. Chen, and K. A. Nelson, Thermal transport in suspended silicon membranes measured by laser-induced transient gratings, *AIP Adv.* **6**, 121903 (2016).
- [57] A. Babuty, K. Joulain, P.-O. Chapuis, J.-J. Greffet, and Y. De Wilde, Blackbody Spectrum Revisited in the Near Field, *Phys. Rev. Lett.* **110**, 146103 (2013).
- [58] G. Bimonte and E. Santamato, General theory of electromagnetic fluctuations near a homogeneous surface in terms of its reflection amplitudes, *Phys. Rev. A* **76**, 013810 (2007).
- [59] G. Bimonte, Scattering approach to Casimir forces and radiative heat transfer for nanostructured surfaces out of thermal equilibrium, *Phys. Rev. A* **80**, 042102 (2009).
- [60] R. Messina and M. Antezza, Scattering-matrix approach to Casimir-Lifshitz force and heat transfer out of thermal equilibrium between arbitrary bodies, *Phys. Rev. A* **84**, 042102 (2011).
- [61] Y. Guo and Z. Jacob, Fluctuational electrodynamics of hyperbolic metamaterials, *J. Appl. Phys.* **115**, 234306 (2014).
- [62] J. A. Kong, *Electromagnetic Wave Theory*, 2nd ed. (Wiley, New York, 1990), pp. 22–25.